Applied Catalysis A: General 520 (2016) 105–113

Contents lists available at ScienceDirect

Applied Catalysis A: General

journal homepage: www.elsevier.com/locate/apcata

Selective etherification of hydroxymethylfurfural to biofuel additives over Cs containing silicotungstic acid catalysts

G. Raveendra, A. Rajasekhar, M. Srinivas, P.S. Sai Prasad, N. Lingaiah*

Catalysis Laboratory, I&PC Division, CSIR-Indian Institute of Chemical Technology, Hyderabad 500007, Telangana, India

ARTICLE INFO

Article history:
Received 27 November 2015
Received in revised form 4 April 2016
Accepted 15 April 2016
Available online 19 April 2016

Keywords:
Silicotungstic acid
Cesium nitrate
Etherification
Ethanol
HMF
EMF

ABSTRACT

A series of Cs exchanged silicotungstic acid (STA) catalysts were prepared and their physico-chemical properties were derived from FT-Infrared, X-ray diffraction, Laser Raman, temperature programmed desorption of ammonia and BET surface area. The characterization results revealed that the Keggin structure of STA remained intact even after Cs ions replaced its protons. The catalysts activity was evaluated for the selective etherification of 5-hydroxymethylfurfural (HMF) with ethanol for the synthesis of 5-ethoxymethylfurfural (EMF). The partial exchange of Cs ions with protons of STA resulted an increase in acidity and the catalysts with two Cs ions in STA showed highest acidity. The activity was explained based on the acidity, surface and structural properties of the catalysts. A detailed study was made on the effect of various reaction parameters such as influence of reaction temperature, reaction time, Cs content on STA to unveil the optimize reaction conditions. The catalyst was recovered easily from the reaction mixture and reused at least four times with constant activity.

1. Introduction

The limited oil resources, as well as economic, geopolitical and environmental reasons indicate that the current petroleum based fuels are unsustainable. Biomass is considered as a sustainable raw material for the production of many chemicals and fuels [1]. Nature produces about 170 billion metric tons of biomass per year by photosynthesis and 75% of which can be assigned to carbohydrates [2,3]. HMF a potential chemical can be obtained from cellulosic biomass such as fructose, glucose, sucrose and inulin [4–7]. HMF can be used to produce 2,5-dimethylfuran (DMF) potential biogasoline compound [8], and 2,5-furandicarboxylic acid (FDCA) a precursor to the polyester, PET [9–11] and 5-ethoxymethylfurfural (EMF), a promising biofuel and fuel additive. Among these chemicals etherification of HMF with ethanol to produce EMF is an important approach as it is an excellent additive for diesel [12]. It has a high energy density of 8.7 kW h L^{-1}, which is comparable with that of standard gasoline (8.8 kW h L^{-1}) and diesel fuel (9.7 kW h L^{-1}), and significantly higher than the widely familiar bio-ethanol (6.1 kW h L^{-1}) [13]. Avantium has used EMF as a blend for commercial diesel in engine tests and found that the engines ran smoothly. Furthermore, there is less solid contamination and soot [14]. EMF may also be hydrogenated over metal catalysts to yield 5-(hydroxyethyl) furfuryl alcohol, which is much more miscible in diesel and has a similar combustion profile to ethanol [15]. Different methods have been reported for the preparation of EMF. EMF have previously been synthesized via 5-chloromethylfurfural with ethanol [16]. Alternatively, EMF has also been synthesized by direct etherification of HMF with ethanol in the presence of acid catalysts such as Amberlyst-131[17], $H_4SiW_{12}O_{40}$/MCM-41, H_2SO_4 [18], ZrO_2/SBA-15[19], Ag_1TPA [20], 40 wt% MCM-41-HPW [21], Fe_3O_4@SiO_2 [22], graphene oxide [23], silica-SO_3H [24], SO_3H-functionalized polymers [25] and cellulose sulfuric acid catalysts [26]. Even though different heterogeneous catalysts are explored for synthesis of EMF, over most of the catalysts activity is limited. The role of catalysts surface and structural characteristics on the etherification activity of HMF is not studied in detailed. Moreover the influence of reaction parameters and reusability of catalysts are not studied in details.

Heteropolyacids (HPAs) have been widely used in the conversion of carbohydrates, especially in the esterification and etherification reactions because of their Brønsted acidity, high proton mobility and the ability to accept and release electrons [27]. HPAs and their salts are useful acid catalysts for diverse reactions that require strong acidity [28]. Although the acid forms are themselves useful solid catalysts, they are highly soluble and difficult to separate from polar media [29]. HPAs grafting onto high-surface area porous support is often used to enhance their

* Corresponding author.
E-mail address: nakkalingaiah.iict@gov.in (N. Lingaiah).

http://dx.doi.org/10.1016/j.apcata.2016.04.017
0926-860X/

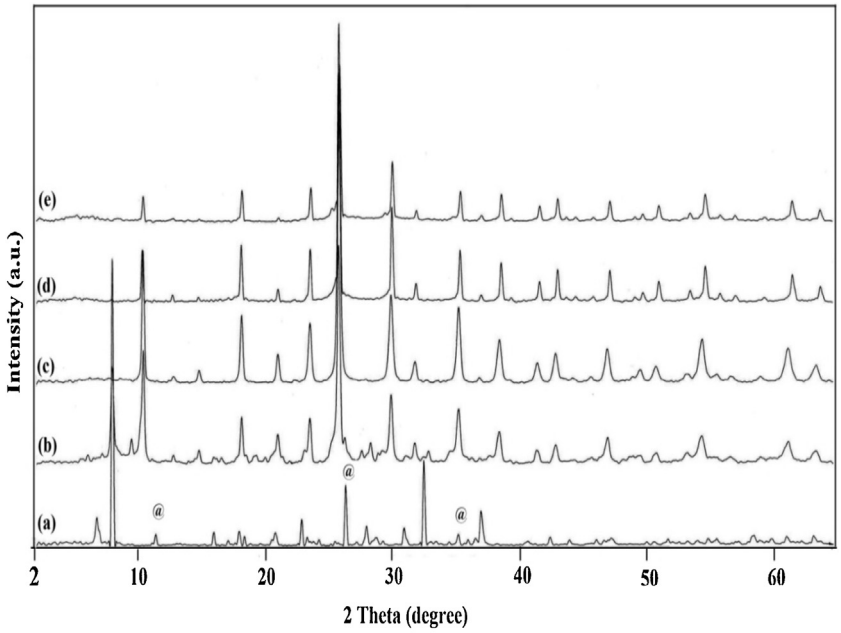

Fig. 1. XRD patterns of CsSTA catalysts (a) STA, (b) Cs_1STA, (c) Cs_2STA, (d) Cs_3STA, (e) Cs_4STA catalysts.

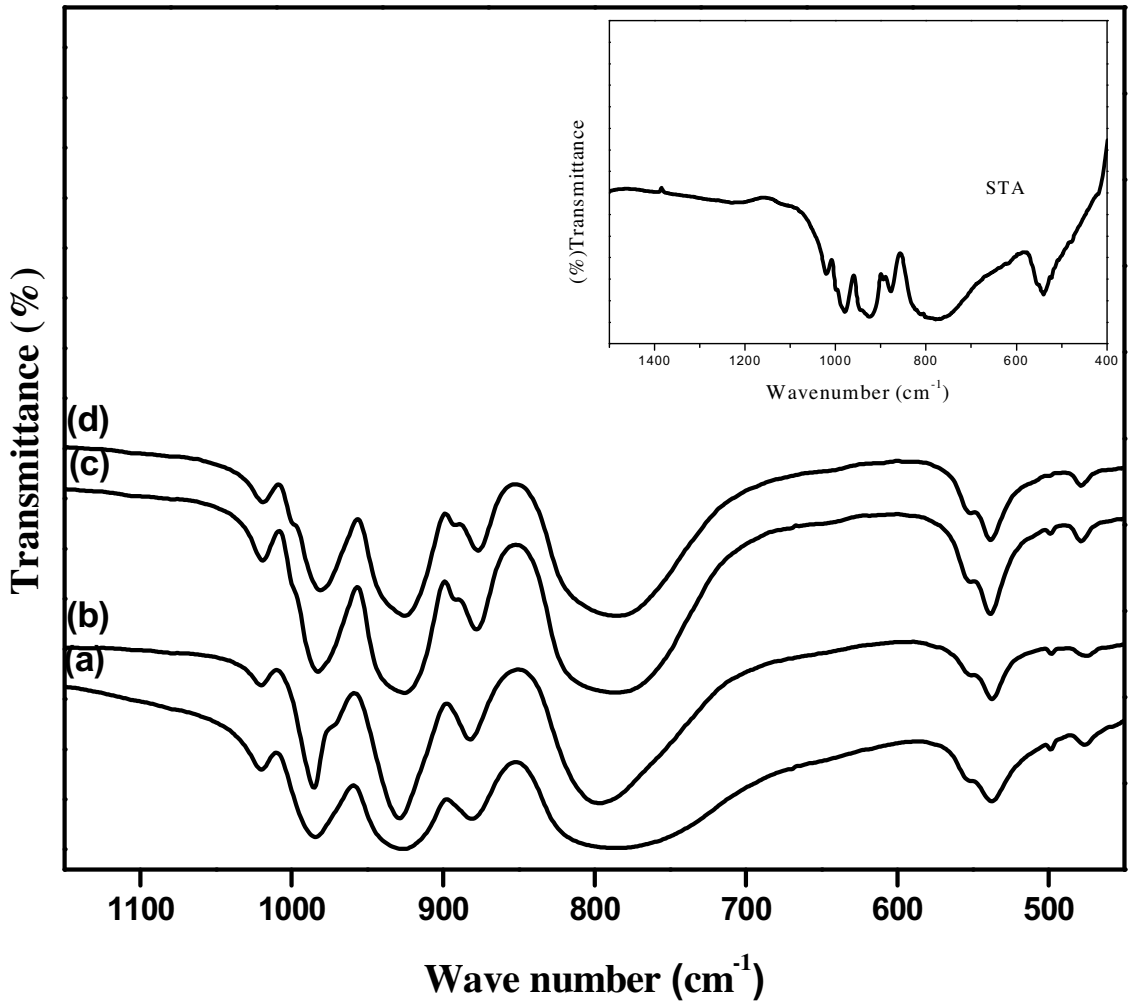

Fig. 2. FT-IR spectra of CsSTA catalysts (a) Cs_1STA (b) Cs_2STA (c) Cs_3STA (d) Cs_4STA, STA (as inserted figure).

Table 1
Physico-chemical properties of CsSTA catalysts.

Catalyst	Cs content taken per Keggin ion (mol)	Actual Cs content per Keggin ion (mol)	Surface area (m^2/g)	Acidity (mmol/g)
STA	–	–	4	1.20
Cs_1STA	1	0.64	85	1.25
Cs_2STA	2	1.70	125	1.30
Cs_3STA	3	2.08	103	1.00
Cs_4STA	4	2.86	79	0.90

[a]Acidity calculated from NH_3-TPD.

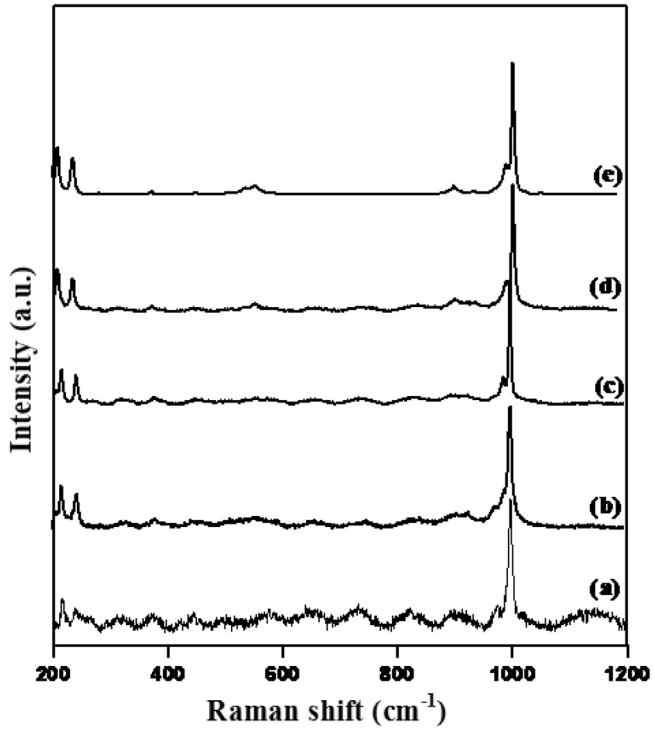

Fig. 3. Raman spectra of CsSTA Catalysts (a) STA (b) Cs_1STA (c) Cs_2STA (d) Cs_3STA (e) Cs_4STA catalysts.

dispersion and accessible acid sites [30]. Alkali-exchanged HPAs (e.g., $Cs_xH_{1-x}PW_{12}O_{40}$) [31] exhibit dramatic increase in surface area and acidity profound changes in solubility over the parent HPA. The salts with large monovalent ions, such as Cs^+, NH^{+4}, and Ag^+, are insoluble in water [32]. Partial substitutions of protons by Cs^+ also change the number of available surface acid sites [33].

The present study related to preparation of Cs salt of silicotungstic acid catalysts for the selective etherification of HMF to yield EMF. These catalysts were characterized by different techniques to derive their surface, structural and acidic properties of the catalysts. The etherification activity was correlated with the characteristics of the catalysts. Establishment of optimum reaction parameters and reusability of the catalysts is also one of the aim of the present study.

2. Experimental

2.1. Catalyst preparation

Cesium exchanged silicotungstic acid (CsSTA) catalysts with varying cesium in the secondary structure of STA were prepared according to the reported procedure [34]. Silicotungstic acid (5 g) was dissolved in 20 mL of deionized water and stirred vigorously at room temperature. Then, the required amount of aqueous solution of $CsNO_3$ was added drop wise to the former solution. The Cs content in $Cs_xH_{4-x}SiW_{12}O_{40}$ (x = 1 to 4) was adjusted using the required amount of Cs. The resultant mixture was aged for 2 h at room temperature and the excess water removed on a hot plate. The obtained solid mass was dried at 120 °C for 12 h and finally calcined at 300 °C for 2 h. Four catalysts were prepared with varying Cs content in $Cs_xH_{4-x}SiW_{12}O_{40}$ (x = 1, 2, 3, 4). These catalysts are denoted as Cs_1STA, Cs_2STA, Cs_3STA and Cs_4STA, where the number indicates the number of Cs ions exchanged with the protons of STA.

2.2. Characterization of catalysts

The FT-IR spectra were recorded on a Bio-Rad Excalibur series spectrometer using the KBr disc method.

The nature of the acid sites (Bronsted and Lewis) of the catalysts was determined by FT-IR spectroscopy with chemisorbed pyridine. The pyridine adsorption studies were carried out in the diffuse reflectance infrared Fourier transform (DRIFT) mode. Prior to the pyridine adsorption catalysts were degassed under vacuum at 200 °C for 3 h followed by suspending dry pyridine. Then, the excess pyridine was removed by heating the sample at 120 °C for 1 h. After cooling the sample to room temperature, FT-IR spectra of the pyridine-adsorbed samples were recorded.

The elemental analysis of the samples was measured by Agilent 7700 Series Inductively Coupled Plasma Mass Spectrometer (ICP-MS).

X-ray powder diffraction patterns were recorded on a Rigaku Miniflex diffractometer using Cu Kα radiation (1.5406 °A) at 40 Kv and 30 mA and secondary graphite monochromatic. The measurements were obtained in steps of 0.045° with count time of 0.5 s in the 2θ range of 10–80°.

Confocal Micro-Raman spectra were recorded at room temperature in the range of 200–1200 cm^{-1} using Horiba Jobin-Yvon Lab Ram HR spectrometer with a 17 mW internal He–Ne (Helium–Neon) laser source of excitation wavelength of 632.8 nm. The catalyst samples in powder form (about 5–10 mg) were usually loosely spread onto a glass slide below the confocal microscope for measurements.

The data on surface area, pore volume and average pore diameter were obtained by nitrogen adsorption at liquid N_2 temperature (–196 °C) using Autosorb-1 (Quanta chrome, USA) instrument. The samples were first out-gassed at 200 °C to ensure a clean surface prior to construction of adsorption isotherms.

Temperature-programmed desorption (TPD) of ammonia was carried out on a laboratory-built apparatus equipped with a gas chromatograph using a thermal conductivity detector (TCD). In a typical experiment, about 0.1 g of oven-dried sample was taken in a quartz tube. Prior to TPD studies, catalyst sample was treated at 300 °C for 1 h by passing pure helium gas (99.9%, 30 mL/min). After pretreatment, the sample was saturated with anhydrous ammonia (10% NH_3-90% He mixture gas) at 100 °C at a flow rate of 30 mL/min for 1 h and was subsequently flushed with He at the same temperature to remove physiosorbed ammonia. The process was continued until a stabilized baseline was obtained in the gas chromatograph. Then, the TPD analysis was carried out from 100 to 800 °C at a heating rate of 10 °C/min. The amount of NH_3 evolved was calculated from the peak area of the already calibrated TCD signal.

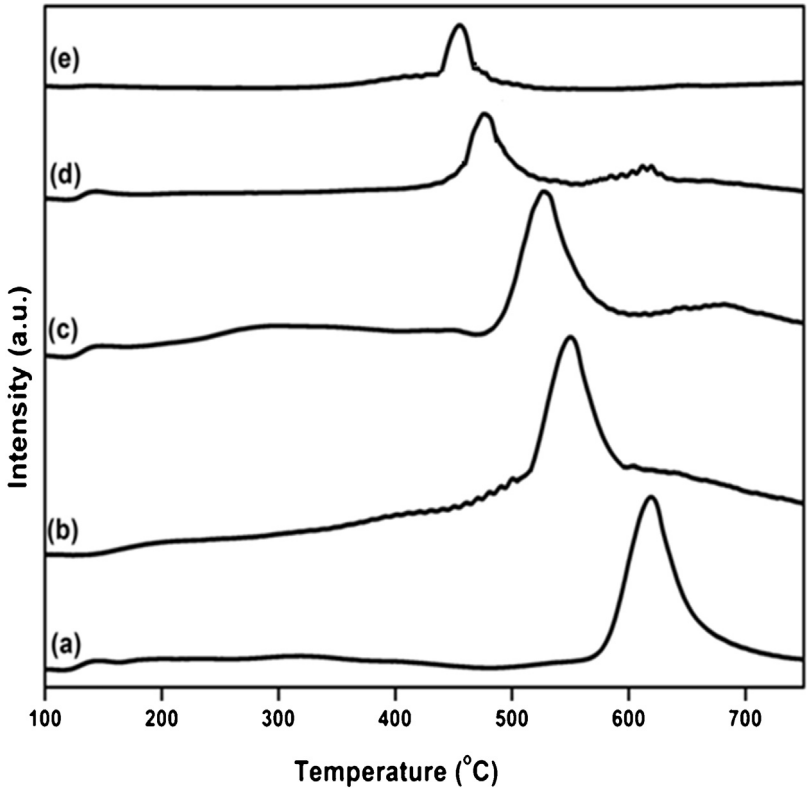

Fig. 4. NH_3-TPD of CsSTA catalysts (a) STA, (b) Cs_1STA, (c) Cs_2STA, (d) Cs_3STA, (e) Cs_4STA catalysts.

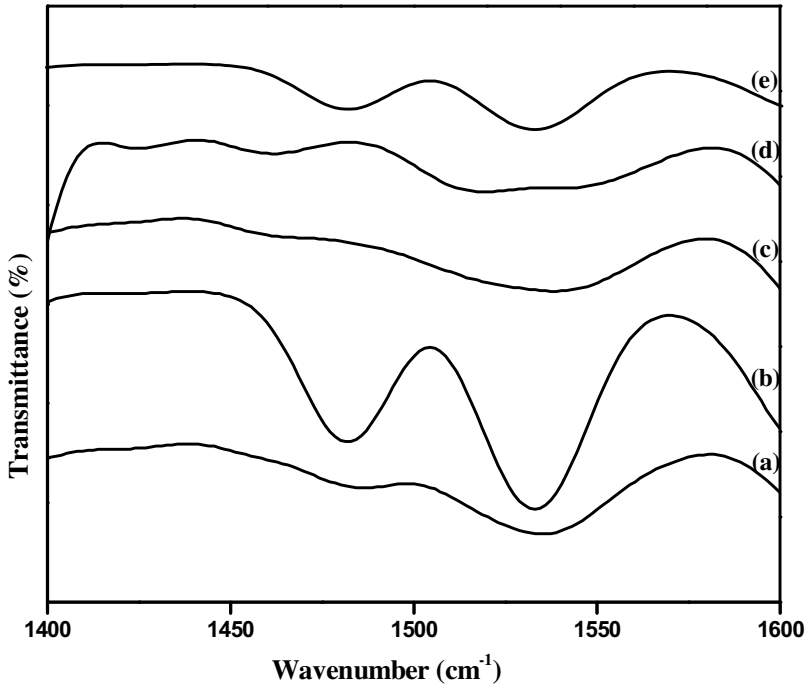

Fig. 5. Pyridine IR spectra of CsSTA catalysts (a) Cs_1STA, (b) Cs_2STA, (c) Cs_3STA, (d) Cs_4STA, (e) Cs_2STA used catalysts.

2.3. General etherification reaction and analysis of products

The etherification reaction was carried out in a 15 mL sealed tube. In a typical run, 0.126 g of HMF was dissolved in 2 g of Ethanol and 0.03 g of catalyst was added. The reaction was carried out at a reaction temperature of 120 °C for 2.5 h. After reaction, the reaction mixture was cooled to room temperature and diluted with ethanol then the catalyst was separated by centrifuge.

The reaction mixture was diluted with absolute ethanol and filtered with a 0.45 μm syringe filter prior to analysis. The products were analyzed by a gas chromatograph (Shimadzu, 2010) equipped with flame ionization detector using innowax capillary column

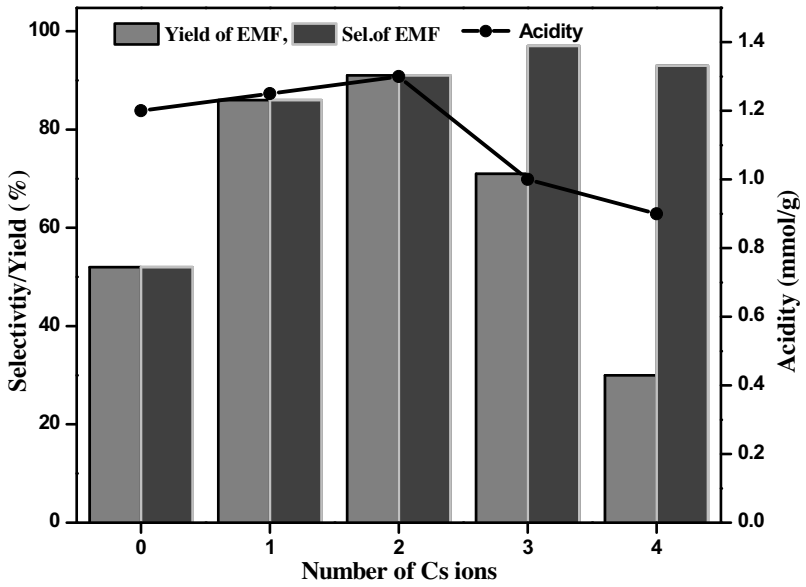

Fig. 6. The influence of Cs content in Cs exchanged STA catalysts on the etherification of HMF. Reaction conditions: HMF (0.126 g), Ethanol (2 g), Catalyst weight (0.03 g), Reaction temperature (120 °C), Reaction time (2.5 h).

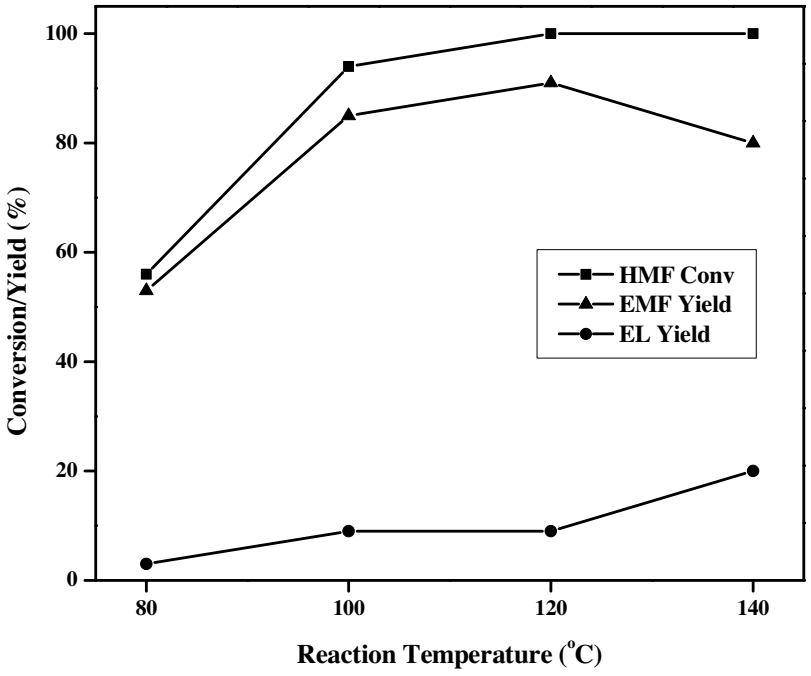

Fig. 7. Effect of reaction temperature on etherification of HMF over Cs_2STA catalyst. Reaction conditions: HMF (0.126 g), Ethanol (2 g), Catalyst weight (0.03 g), Reaction temperature (80–140 °C), Reaction time (2.5 h).

(diameter: 0.25 mm, length 30 m). Products were also identified by GC–MS (Shimadzu, GCMS-QP2010S) analysis.

3. Results and discussion

3.1. Catalyst characterization

BET surface area values of cesium exchanged silicotungstic acid catalysts are summarized in Table 1. The actual amount of Cs exchanged with the protons of STA Keggin ion were also measured and showed in this table. The surface areas of the catalysts increased with increase in cesium content in STA. The increase in surface area is related to the change in morphology corresponding to the formation of small spherical shaped particles obtained by precipitation of Cs salts of STA [35]. This could be interpreted that the large Cs ions widen the interstitial volume between Keggin units and create new pores [36]. The presence of large sizes of metal cation such as Cs increases the cubic lattice parameters of heteropolyacid. This results an increased mesoporosity of these solids [37]. When the Cs content increased from Cs_3STA to Cs_4STA these mesopores due to the higher crystalline the surface area decreases.

Fig. 1 illustrates the XRD patterns of parent STA and CsSTA catalysts. Bulk STA showed five main diffraction peaks at 2θ values of 8, 11.3, 26.5 33 and 34.7° which can be assigned to the characteristic peaks of body centred cubic secondary structure of Keggin ion. In the case of cesium exchanged STA catalysts the same diffrac-

tion patterns were observed with a marginal shift towards lower 2θ values indicating an increase in the unit cell volume [38,39]. The shift of peaks particularly observed at a 2θ value of 26.5° for the Cs exchanged STA catalysts. This is due to the formation of dihydronium ions ($H_5O_2^+$) caused due to the exchange of acidic protons present in the secondary heteropoly structure by Cs^+ ions. The hydrated cesium cation is responsible for the separation of d-spacing [40]. The intensity of the characteristic diffraction peaks of STA decreased with the increase in cesium content.

FT-IR spectra of Cs exchanged STA catalysts are shown in Fig. 2. Bulk STA showed the characteristic infrared frequencies at 1020, 979, 875 and 778 cm^{-1} related to Si—O, oxygen in central SiO_4 tetrahedron, W = O terminal oxygen bonding to W, inter-octahedral W—O—W and intra-octahedral W–O–W respectively [34,41]. These characteristic bands were found in the spectra of cesium exchanged STA catalysts. The presence of characteristic IR spectra of Keggin ions for these catalysts indicate that the Keggin structure is intact during the exchange of protons in the secondary structure of STA with cesium ions.

Raman spectra of STA and its cesium exchanged catalysts are shown in Fig. 3. STA showed Raman bands at 998, 974, 850 cm^{-1} which are attributed to $W = O_t$ stretching vibration, W—O—W bending, W—O—W stretching vibrations respectively [42]. The band observed at 555 cm^{-1} is associated with O—Si—O bending vibration. The band at 243 cm^{-1} corresponds to the W—O—W bending mode of intact Keggin ion. All these characteristic Raman bands observed for cesium salts of STA, indicated that the Keggin structure of STA was not affected, even after exchange of its protons with cesium. The results drawn from the Raman spectroscopy are in support with the observations made from FT-IR and XRD.

The ammonia adsorption–desorption technique usually enables for the determination of strength of acid sites present on the catalyst surface together with total acidity. Generally the strength of solid acid sites with TPD profiles can be classified into three types based on the desorption temperature. They are classified as weak (150–300 °C), moderate (300–500 °C) and strong acidic sites (500–650 °C) [43]. TPD patterns of the catalysts are shown in Fig. 4. The acidity of the catalysts were calculated and presented in Table 1. In the case of pure STA a desorption peak in the temperature range of 550–750 °C was observed. When its proton was partially exchanged with cesium ions an increase in total acidity was observed. An increase in cesium content in the secondary structure of STA (Cs_2STA) the ammonia desorption peak shifted to lower temperature. Thus indicates a decrease in the strong acidic sites. Further increase of cesium content, as in the case of Cs_3STA, the desorption peak is low. On the other hand, Cs_4STA catalyst exhibited further low TPD desorption peak. The absence of NH_3 desorption peak at high temperature in case of Cs_4STA catalyst might be due to complete exchange of STA protons with cesium ion. Partially exchanged Cs_2STA catalyst exhibited high acidity in contrast to the fully exchanged catalysts. The partially exchanged catalyst exhibits high acidity due to the mobility of residual protons in the secondary structure of STA [44].

Pyridine adsorbed FT-IR spectra of cesium salts of STA catalysts are shown in Fig. 5. The pyridine–adsorbed FT-IR spectra showed various features in the region of 1400–1600 cm^{-1} due to the stretching vibrations of M–N (metal–nitrogen) and N—H (pyridinium ion). The FT–IR spectra of the catalysts showed prominent bands at 1534 and 1481 cm^{-1}. These IR band observed are assigned to characteristic protonation of pyridine molecule onto Brønsted acidic sites. Heteropoly trungstate shows typically intense IR bands at 1530 and 1542 cm^{-1} characteristic of Brønsted acidic sites [45]. The absence of band related to Lewis acidic sites at 1441 cm^{-1} suggests the absence of Lewis acidic sites in the Cs containing TPA catalysts. The high intensity of the IR bands for the partially exchanged Cs_2STA catalyst suggests the presence of large amount of Brønsted acidic sites. These stronger Brønsted sites are might be generated due to higher proton mobility of residual protons than the fully exchanged Cs_4STA [46]. The mobility of residual protons for the partially substituted HPAs is high and results in increased Brønsted acidity. The pyridine adsorbed FT-IR results suggest that the Cs containing STA catalysts are possessing Brønsted acidic sites only.

3.2. Catalytic activity of CsSTA catalysts for etherification of HMF

3.2.1. Influence of cs content in Cs exchanged STA catalysts on HMF etherification

Etherification of HMF was carried over Cs exchanged STA catalysts and the results are shown in Fig. 6. The yield of EMF and selectivity was plotted against the number of Cs ions in STA. In Keggin type heteropolyacids STA is one of the Brønsted acid and exhibited 52% of EMF yield. Although STA showed reasonable activity, it is homogeneous as it is highly soluble in polar solvents. The cesium salts of STA which are insoluble showed very good catalytic activity as compared to pure STA. The etherification of HMF increased with an increase of the cesium content in the secondary structure of STA, where the catalyst Cs_2STA exhibited about 91% yield of EMF. The activity decreased for the catalyst with more than two Cs ions in STA. Complete exchange of Cs ions with the protons of STA (Cs_4STA) exhibited very low activity towards etherification of HMF. The activity of the catalysts can be correlated with their physico-chemical characteristics. Bulk STA showed low surface area and Cs exchanged STA catalysts surface area is high. The exchange of Cs ions also led to substantial increase in surface area and acidity of the catalysts. The activity of the catalysts was directly related to largely available acidic sites. Cs_3STA catalyst exhibited about 71% of EMF yield and the Cs_4STA showed only 30% yield of EMF. These results indicated that the etherification of HMF required acidic sites of the catalysts. The low activity of Cs_4STA catalyst might be related to its low acidity which is due to absence of residual protons. These results indicate that the etherification activity is mainly controlled by the relative number of available surface acid sites. These sites are boosted by the higher surface area and porosity due to Cs ions exchange with the protons of STA. Similar observation were reported by Narasimharao et al. [47] on Cs exchanged heteroply tungstate for the acid catalyzed reactions.

3.2.2. Effect of reaction temperature

As the Cs_2STA catalyst exhibited highest activity it is selected as system catalyst and studied to optimise reaction conditions. The effect of reaction temperature over Cs_2STA catalyst on etherification of HMF was investigated at different temperature in the range 80–140 °C and the results are presented in Fig. 7. The reaction temperature played a significant role on EMF yield. When the reaction was conducted at 80 °C the EMF yield was only 50%. Further increase in temperature from 80 to 120 °C the EMF yield increased upto 91%. A marginal decrease in the yield of EMF was observed when the reaction carried at 140 °C. At this temperature formation of by product EL was observed. This indicates that at high reaction temperature etherification of EMF to EL takes place. The optimum reaction temperature for selective formation of EMF is 120 °C.

3.2.3. Effect of reaction time

The effect of reaction time on the etherification of HMF was studied and the results are shown in Fig. 8. The catalyst showed reasonable activity within 1 h. Increase in reaction time led to marginal increase in the yield of EMF. The EMF yield was 91% after 2.5 h. When the reaction time was extended beyond 2.5 h almost there was no further increase in the yield of EMF. However a marginal decrease in selectivity towards EMF was observed at high reaction times. This indicates that with increase in reaction time EMF under

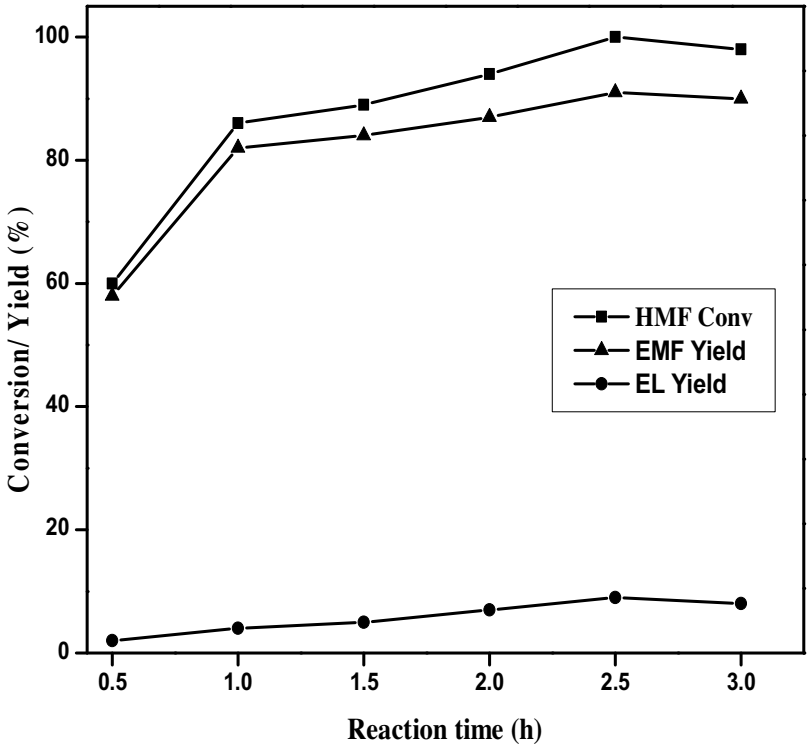

Fig. 8. Influence of reaction time on etherification of HMF over Cs_2STA catalyst. Reaction conditions: HMF (0.126 g), Ethanol (2 g), Catalyst weight (0.03 g), Reaction temperature (120 °C), Reaction time (0.5–3 h).

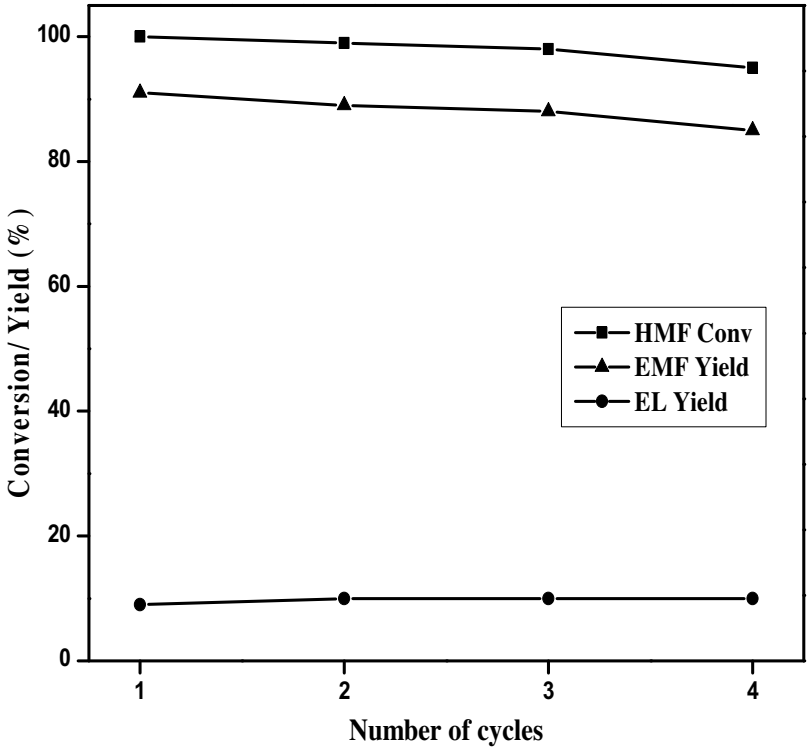

Fig. 9. Recyclability of Cs_2STA catalyst for etherification of HMF. Reaction conditions: HMF (0.126 g), Ethanol (2 g), Catalyst weight (0.03 g), Reaction temperature (120 °C), Reaction time (2.5 h).

Table 2
Synthesis of EMF from HMF catalyzed by various solid acid catalysts.

Catalyst	Temperature (°C)	Time (h)	HMF conversion (%)	EMF Yield (%)	Ref.
$H_4SiW_{12}O_{40}$/MCM-41	90	4	92.0	84.2	[18]
ZrO_2/SBA-15	140	5	100	76	[19]
Ag_1TPA	100	10	93.0	86.6	[20]
40 wt% MCM-41-HPW	100	12	96.1	83.4	[21]
Fe_3O_4@SiO_2	100	11	89.5	76.9	[22]
GO	100	10	100	92	[23]
Silica-SO_3H catalyst	100	10	96.5	83.8	[24]
H_2SO_4	90	2	50.3	34.5	[18]
Cs_2STA	120	2.5	100	91	Present work

goes ethanolysis to yield EL. These results indicate that the optimal reaction time is 2.5 h for etherification of HMF with ethanol on Cs_2STA catalyst.

3.2.4. Comparison with other solid acid catalysts

The performance of present Cs_2STA catalyst was compared with other reported solid acid catalysts for etherification of HMF [20–26]. The results are summarized in Table 2. The Table $H_4SiW_{12}O_{40}$/MCM-41 catalysts showed about 84% yield of EMF after 2.5 h reaction. Silver exchanged tungstophosphoric acid (Ag_1TPA) catalyst gave EMF yield of 86% at a reaction temperature of 100 °C after 10 h. The mesoporous MCM-41 supported on TPA catalysts exhibited 83% EMF yield within 12 h. The formation of EMF from HMF products depends considerably on the nature of the catalyst. The reported solid acid catalysts gave considerable EMF yield at relatively high reaction times compared to present Cs_2STA catalysts. The present Cs_2STA catalysts gave about 91% yield with in short reaction time of 2.5 h compared to other reported catalysts.

3.2.5. Reusability of Cs_2 STA catalyst

Reusability is an important characteristic of heterogeneous catalysts which can reduce the cost of the process. In order to study the reusability of Cs_2STA catalyst, the used catalyst was separated from reaction mixture by centrifugation after completion of the reaction. The obtained catalyst was washed with ethanol, dried at 100 °C prior to its reuse for further reaction cycle under the identical reaction conditions. The reusability of Cs_2STA catalyst was studied for four times and the results are shown in Fig. 9. The amount Cs present in the used catalysts was measured. The amount of Cs in the used content is 1.68 mol compared to 1.70 mol of Cs content in virgin catalyst. This indicates that the leaching of Cs is negligible during the reaction. A slight decrease in the yield of EMF is noticed, which may be due to blockage of acidic sites and marginal loss of catalyst during the reaction. These results clearly indicate that the Cs_2STA catalyst was stable during the reaction and could be reused without significant loss in its catalytic activity.

4. Conclusions

Cesium-exchanged silicotungstic acid catalysts with retention of Keggin ion structure were prepared and studied for etherification of HMF. The activity of the catalysts depended on the number of protons exchanged with Cs ion. The presence of Cs ions led to substantial increase in surface area and acidity of the catalysts. The catalyst with two Cs ions exchanged with STA (Cs_2STA) showed highest activity. The Cs_2STA catalyst showed about 91% yield of EMF at 120 °C with in 2.5 h. Different reaction parameters such as effect of reaction temperature, catalyst weight and reaction times were studied and optimum conditions were established. The Cs_2STA catalyst is reusable without any pretreatment with consistent etherification activity.

Acknowledgments

The authors thank to Council of Scientific & Industrial Research (CSIR), New Delhi, India for the financial support in the form of Catalysis for Specialty Chemicals (CSC-0125) project under 12th Five Year Programme. The authors thank to Dr. R. Srinivas, Head Analytical division, IICT, India, for their kind help with the ICP-OES Analysis.

References

[1] S.E. Davis, L.R. Houk, E.C. Tamargo, A.K. Datye, R.J. Davis, Catal. Today 160 (2011) 55–60.
[2] P. Wang, H.B. Yu, S.H. Zhan, S.Q. Wang, Bioresour. Technol. 102 (2011) 4179–4183.
[3] J.C. Serrano-Ruiz, J.A. Dumesic, Energy Environ. Sci. 4 (2011) 83–99.
[4] T. Deng, X. Cui, Y. Qi, Y. Wang, X. Hou, Y. Zhu, Chem. Commun. 48 (2012) 5494–5496.
[5] A.A. Rosatella, S.P. Simeonov, R.F.M. Frade, C.A.M. Afonso, Green Chem. 13 (2011) 754–793.
[6] G. Raveendra, M. Srinivas, N. Pasha, A.V. Prasada Rao, P.S. Sai Prasad, N. Lingaiah, React. Kinet Mech. Cat. 115 (2015) 663–678.
[7] G. Raveendra, M. Srinivas, P.S. Sai Prasad, N. Lingaiah, Int. J. Adv. Eng. Sci. Appl. Math. 5 (4) (2013) 232–238.
[8] O. Casanova, S. Iborra, A. Corma, J. Catal. 265 (2009) 109–116.
[9] P. Walt, G.V. Vladimir, Adv. Synth. Catal. 343 (2001) 102–111.
[10] C.A. Mullen, A.A. Boateng, ACS Sustain. Chem. Eng. 3 (2015) 1623–1631.
[11] Y. Román-Leshkov, C.J. Barrett, Z.Y. Liu, J.A. Dumesic, Nature 447 (2007) 982–985.
[12] H. Wang, T. Deng, Y. Wang, Y. Qi, X. Hou, Y. Zhu, Bioresour. Technol. 136 (2013) 394–400.
[13] B. Liu, Z. Zhang, RSC Adv. 3 (2013), 12313–1123.
[14] G. J. M. Gruter, F. Dautzenberg, U.S. Patent Appl. 2011/0082304 A1 (2011).
[15] E.J. Ras, S. Maisuls, P. Haesakkers, G.J. Gruter, G. Rothenberg, Adv. Synth. Catal. 351 (2009) 3175–3185.
[16] M. Mascal, E.B. Nikitin, Angew. Chem. Int. Ed. 47 (2008) 7924–7926.
[17] C.M. Lew, N. Rajabbeigi, M. Tsapatsis, Ind. Eng. Chem. Res. 51 (14) (2012) 5364–5366.
[18] P.H. Che, F. Lu, J.J. Zhang, Y.Z. Huang, X. Nie, J. Gao, J. Xu, Bioresour. Technol. 119 (2012) 433–436.
[19] P. Lanzafame, D.M. Temi, S. Perathoner, G. Centi, A. Macario, A. Aloise, G. Giordano, Catal. Today. 175 (2011) 435–441.
[20] Y. Ren, B. Liu, Z. Zhang, J. Lin, J. Ind. Eng. Chem. 21 (2015) 1127–1131.
[21] A. Liu, Z. Zhang, Z.F. Fang, B. Liu, K. Huang, J. Ind. Eng. Chem. 20 (2014) 1977–1984.
[22] S.G. Wang, Z.H. Zhang, B. Liu, J.L. Li, Catal. Sci. Technol. 3 (2013) 2104–2112.
[23] H. Wang, T. Deng, Y. Wang, X. Cui, Y. Qi, X. Mu, X. Hou, Y. Zhu, Green Chem. 15 (2013) 2379–2383.
[24] B. Liu, Z. Zhang, RSC Adv. 3 (2013) 12313–12319.
[25] H. Li, Q. Zhang, S. Yang, Ind. J. Chem. Eng. 2014 (2014) 1–7.
[26] B. Liu, Z. Zhang, K. Huang, Cellulose 20 (2013) 2081–2089.
[27] I.V. Kozhevnikov, Chem. Rev. 98 (1998) 171–198.
[28] N. Mizuno, M. Misono, Chem. Rev. 98 (1998) 199–218.
[29] T. Okuhara, N. Mizuno, M. Misono, Adv. Catal. 41 (1996) 113–252.
[30] M. Misono, Catal. Rev. Sci. Eng. 29 (1987) 269–321.
[31] T. Okuhara, T. Nishimura, H. Watanabe, M. Misono, J. Mol. Catal. 74 (1992) 247–256.
[32] T. Okuhara, T. Arai, T. Ichiki, K.Y. Lee, M. Misono, J. Mol. Catal. 55 (1989) 293–301.
[33] N. Mizuno, M. Misono, Chem. Lett. 16 (1987) 967–970.
[34] S. Borghese, A. Blanc, P. Pale, B. Louis, Dalton Trans. 40 (2011) 1220–1223.
[35] K. Srilatha, R. Sree, B.L.A. Prabhavathi Devi, P.S. Sai Prasad, R.B.N. Prasad, N. Lingaiah, Bioresour. Technol. 116 (2012) 53–57.
[36] A. Corma, A. Martínez, C. Martínez, J. Catal. 164 (1996) 422–432.
[37] G.B. Mc Garvey, J.B. Moffat, J. Catal. 130 (1991) 483–497.

[38] A. Vakulenko, Y. Dobrovolsky, L. Leonova, A. Karelin, A. Kolesnikova, N. Bukun, Solid State Ion. 136 (7) (2000) 285–290.
[39] L.W. Lan, J. Li, Q.Y. Chen, Nonferrous Metals 3 (2009) 35–38.
[40] L.R. Pizzio, M.N. Blanco, Microporous Mesopororous Mater. 103 (2007) 40–47.
[41] K.T. VenkateswaraRao, P.S. Sai Prasad, N. Lingaiah, Green Chem. 14 (2012) 1507–1514.
[42] B.M. Devassy, S.B. Halligudi, J. Catal. 236 (2005) 313–323.
[43] L. Shen, H. Yin, A. Wang, Y. Feng, Y. Shen, Z. Wu, T. Jiang, Chem. Eng. J. 180 (2012) 277–283.
[44] M.H. Haider, N.F. Dummer, D. Zhang, P. Miedziak, T.E. Davies, S.H. Taylor, D.J. Willock, D.W. Knight, D. Chadwick, G.J. Hutchings, J. Catal. 286 (2012) 206–213.
[45] K. Jagadeeswaraiah, Ch. Ramesh Kumar, P.S. Sai Prasad, N. Lingaiah, Catal. Sci. Technol. 4 (2014) 2969–2977.
[46] Ch. Ramesh Kumar, K.T. Venkateswara Rao, P.S. Sai Prasad, N. Lingaiah, J. Mol. Catal. A. 337 (2011) 17–24.
[47] K. Narasimharao, D.R. Brown, A.F. Lee, A.D. Lee, A.D. Newman, P.F. Siril, S.J. Tavener, K. Wilson, J. Catal. 248 (2007) 226–234.